

Majorana Fermions in Proximity-coupled Topological Insulator Nanowires

A. Cook and M. Franz¹

¹*Department of Physics and Astronomy, University of British Columbia, Vancouver, BC, Canada V6T 1Z1*

A finite-length topological insulator nanowire, proximity-coupled to an ordinary bulk s -wave superconductor and subject to a longitudinal applied magnetic field, is shown to realize a one-dimensional topological superconductor with unpaired Majorana fermions localized at both ends. This situation occurs under a wide range of conditions and constitutes what is possibly the most easily accessible physical realization of the elusive Majorana particle in a solid-state system.

Predicted in a seminal 1937 paper¹ as purely real (as opposed to complex-valued) solutions of the Dirac equation describing a spin- $\frac{1}{2}$ particle, Majorana fermions are distinguished by the curious fact that they are their own anti-particles. More precisely, in second quantized formulation, the creation and annihilation operators for Majorana fermions coincide. In high-energy physics compelling theoretical arguments suggest that neutrinos might be Majorana fermions but a convincing experimental proof is yet to be given². In condensed matter physics Majorana fermions can appear as *emergent* degrees of freedom in certain systems of electrons when superconducting order or strong correlations are present^{3,4}. Over the past decade solid state realizations of Majorana fermions have been under intense theoretical study both as a fundamental intellectual challenge and as a possible platform for fault-tolerant quantum computation^{5,6}. Yet their remarkable properties – and indeed their very existence – await experimental confirmation.

The purpose of this Communication is to advance a proposal for a new type of solid-state device that can serve as a host for Majorana fermions under a wide range of experimentally accessible conditions. Our proposed device, depicted schematically in Fig. 1, draws conceptually on recent ideas to realize Majoranas in both two- and one-dimensional heterostructures composed of a topological insulator⁷ or a semiconductor with strong spin-orbit coupling^{8–11}, coupled to an ordinary superconductor through a proximity effect. Specifically, we consider a nanowire (i.e. quantum wire with nanometer-scale cross-section) fashioned out of a strong topological insulator (STI), such as Bi_2Se_3 or $\text{Bi}_2\text{Te}_2\text{Se}$, placed on top of an ordinary s -wave superconductor (SC), subject to applied magnetic field along the axis of the nanowire. Through a combination of analytical insights and numerical calculations we demonstrate below that when the magnetic flux through the nanowire cross-section is close to a half-integer multiple of the fundamental flux quantum $\Phi_0 = hc/e$, the topologically protected surface state realizes a one-dimensional *topological superconductor*¹² with Majorana fermions localized near the ends of the wire. We note that single-crystalline Bi_2Se_3 nanowires with ribbon geometry (i.e. ‘nanoribbons’) have been fabricated¹³ and transport experiments in these show unambiguous evidence for the topologically protected surface states up to, possibly, a room temperature¹⁴. Very recently, the SC proximity effect has been demonstrated

in $\text{Sn-Bi}_2\text{Se}_3$ interfaces¹⁵.

The device depicted in Fig. 1 appears superficially similar to the devices based on semiconductor wires proposed in Refs.^{10,11}. The physics underlying the emergence of Majorana fermions is nevertheless fundamentally different. In the semiconductor wires the applied magnetic field serves to open up a gap through the Zeemann coupling to electron spins whereas our proposal relies exclusively on the orbital effect of the applied field. This difference leads to several key advantages of our device over the previous proposals. First, for the topological phase to occur in a semiconductor wire it is essential that the chemical potential is fine-tuned to lie inside the Zeemann gap, whose typical size in 1T field is ~ 1 meV or less. In our device, by contrast, chemical potential can be anywhere inside the TI bulk gap, which is ~ 300 meV in Bi_2Se_3 . Second, as explained below, our device can be operated in the regime where the TI surface state is protected by time reversal symmetry (\mathcal{T}) and the induced pairing gap is therefore robust against non-magnetic disorder. Such a protection is absent in ordinary semiconductor wires^{10,11}. Finally, the energy gap protecting the Majorana fermions in our setup is generically an order of magnitude larger than in previous proposals.

We begin with a qualitative discussion of the physics behind the proposed device. As explained in previous works^{7,12} the key ingredient necessary to build a topological superconductor is an underlying normal state characterized by the electron dispersion with the spin degeneracy removed. It is possible to achieve this situation on the surface of a TI^{16–18}. The low-energy fermionic excitations on such a surface are governed by the Dirac

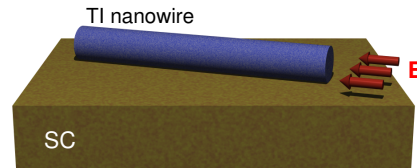


FIG. 1: Schematic of the proposed device. Magnetic field \mathbf{B} is applied along the axis of the wire taken to coincide with the z -direction.

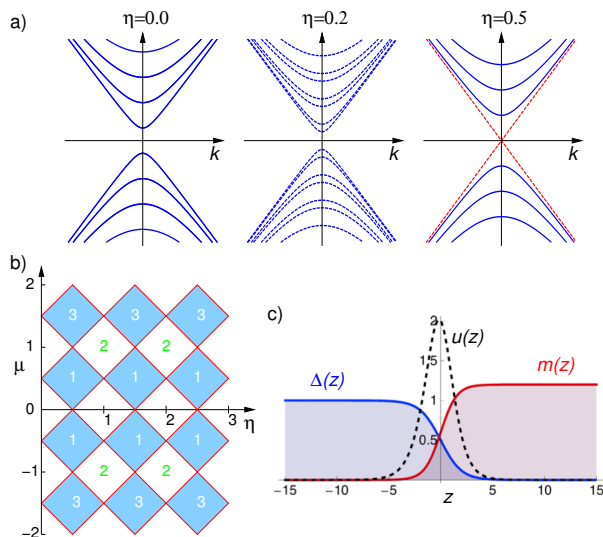


FIG. 2: a) Surface state excitation spectra E_{kl} for various values of magnetic flux $\Phi = \eta\Phi_0$. Solid and dashed lines indicate doubly degenerate and non-degenerate bands, respectively. b) Kitaev's Majorana number: $\mathcal{M} = -1(+1)$ in shaded (white) regions. Numerals inside the squares indicate the number of Fermi points for $k > 0$. c) A possible shape of SC/magnetic domain wall located near $z = 0$. Dashed line shows the exact zero-mode solution $u(z)$ for this domain wall.

Hamiltonian¹⁹

$$h = \frac{1}{2}v[\hbar\nabla \cdot \hat{\mathbf{n}} + \hat{\mathbf{n}} \cdot (\mathbf{p} \times \mathbf{s}) + (\mathbf{p} \times \mathbf{s}) \cdot \hat{\mathbf{n}}] + \mathbf{s} \cdot \mathbf{m}, \quad (1)$$

where $\mathbf{p} = -i\hbar\nabla$, v is the Dirac velocity, $\hat{\mathbf{n}}$ unit vector normal to the surface, and $\mathbf{s} = (s_1, s_2, s_3)$ the vector of Pauli spin matrices. \mathbf{m} denotes the magnetization vector, caused e.g. by the Zeemann coupling of spins to the external magnetic field. Inclusion of the latter is not essential for the functionality of the proposed device but will prove useful in subsequent considerations.

Now consider a TI wire in the shape of a cylinder with radius R and magnetic field \mathbf{B} applied along its axis. The magnetic flux is included by replacing the momentum operator with $\boldsymbol{\pi} = \mathbf{p} - (e/c)\mathbf{A}$, where $\mathbf{A} = \eta\Phi_0(\hat{z} \times \mathbf{r})/2\pi r^2$ is the vector potential. $\Phi = \eta\Phi_0$ represents the total magnetic flux through the cylinder. Taking $\hat{\mathbf{n}} = (\cos\varphi, \sin\varphi, 0)$ and $\mathbf{m} = 0$ the spectrum of Hamiltonian (1) reads²⁰

$$E_{kl} = \pm v\hbar\sqrt{k^2 + \frac{(l + \frac{1}{2} - \eta)^2}{R^2}}. \quad (2)$$

Here k labels momentum eigenstates along the cylinder while $l = 0, \pm 1, \dots$ is the angular momentum. The spectrum in Eq. (2) is clearly periodic in η which reflects the expected Φ_0 -periodicity in the total flux. Our identification of the suitable ‘spinless’ normal state hinges on the following observation. For $\eta = 0$ all branches of E_{kl} are doubly degenerate (Fig. 2a). For $\eta \neq 0$, however,

the degeneracy is lifted and one can always find a value of the chemical potential μ that yields a *single pair* of non-degenerate Fermi points, as illustrated in Fig. 2a. Pairing induced by the proximity effect in such a state is then expected to drive the system into a topological phase.

One can formalize the above argument by considering Kitaev's Majorana number \mathcal{M} defined as $\mathcal{M} = (-1)^\nu$, where ν represents the number of Fermi points for $k > 0$. In the limit of weak pairing, $\mathcal{M} = -1$ indicates the existence of unpaired Majorana fermions at the ends of the wire¹². Fig. 2b shows \mathcal{M} calculated from the spectrum Eq. (2) as a function of μ and η . We observe, specifically, that when $\eta = 1/2$, i.e. for the flux equal to half-integer multiple of Φ_0 , Majorana fermions will appear for *any* value of the chemical potential (as long as it lies inside the bulk gap). This result is easily understood by noting that for $\eta = 1/2$ the gapless $l = 0$ branch is non-degenerate while the remaining branches are all doubly degenerate. Thus, the number of Fermi points for $k > 0$ is odd for any value of μ . It is also worth noting that, for the surface state, $\eta = 1/2$ represents a \mathcal{T} -invariant point and the above pattern of degeneracies should therefore be robust with respect to non-magnetic disorder^{21–23}. In this situation Cooper pairs are formed from time-reversed electron states and the pairing gap is protected against disorder by Anderson's theorem. Below, we will explicitly demonstrate the existence and the robustness of the Majorana fermions both analytically within the low-energy theory based on Hamiltonian (1) and numerically using a minimal lattice model.

Writing the Hamiltonian (1) in cylindrical coordinates and with the ansatz for the wavefunction

$$\psi_{kl}(z, \varphi) = e^{i\varphi l} e^{-ikz} \begin{pmatrix} f_{kl} \\ e^{i\varphi} g_{kl} \end{pmatrix} \quad (3)$$

the spinor $\tilde{\psi}_{kl} = (f_{kl}, g_{kl})^T$ is an eigenstate of

$$\tilde{h}_{kl} = s_2 k + s_3 [l + \frac{1}{2} - \eta]/R + m]. \quad (4)$$

Here we take $v = \hbar = 1$ and $\mathbf{m} = m\hat{z}$. To illustrate the emergence of Majorana fermions in the simplest possible setting we now focus on the $\eta = 1/2$ case and consider chemical potential $|\mu| < v\hbar/R$, i.e. intersecting only the $l = 0$ branch of the spectrum Eq. (2). The Hamiltonian for this branch then becomes $h_k = (ks_2 - \mu) + ms_3$, where we have explicitly included the chemical potential term.

With this preparation we can now construct the Bogoliubov-de Gennes Hamiltonian describing the proximity-induced superconducting order in the nanowire. In the second-quantized notation it reads $H = \sum_k \Psi_k^\dagger \mathcal{H}_k \Psi_k$ with $\Psi_k = (f_k, g_k, f_{-k}^\dagger, g_{-k}^\dagger)^T$ and

$$\mathcal{H}_k = \begin{pmatrix} h_k & \Delta_k \\ -\Delta_k^* & -h_{-k}^* \end{pmatrix}. \quad (5)$$

In the following we consider the simplest s -wave pair potential $\Delta_k = \Delta_0 i s_2$ with Δ_0 a (complex) constant order parameter, which corresponds to the pairing term

$\Delta_0(f_k^\dagger g_{-k}^\dagger - g_k^\dagger f_{-k}^\dagger)$. Introducing Pauli matrices τ_α in the Nambu space we can write, assuming Δ_0 real,

$$\mathcal{H}_k = \tau_3(s_2 k - \mu + s_3 m) - \tau_2 s_2 \Delta_0, \quad (6)$$

with eigenvalues $E_k = \pm[k^2 + \mu^2 + m^2 + \Delta^2 \pm 2(k^2 \mu^2 + \mu^2 m^2 + m^2 \Delta^2)^{1/2}]^{1/2}$.

In the special case when $\mu = 0$ the spectrum simplifies,

$$E_k = \pm\sqrt{k^2 + (m \pm \Delta_0)^2}. \quad (7)$$

The form of the spectrum above suggests that a localized zero-mode will exist at a boundary between SC and magnetic domains, i.e. when $(m \pm \Delta_0)$ changes sign. We thus seek a zero-energy eigenstate $\mathcal{H}\Psi_0(z) = 0$ of $\mathcal{H} = \tau_3[-s_2 i \partial_z + s_3 m(z)] - \tau_2 s_2 \Delta(z)$ with $m(z)$, $\Delta(z)$ of the form indicated in Fig. 2c. A single Jackiw-Rossi zero mode²⁴ indeed exists and has the form $\Psi_0(z) = (1, -1, 1, -1)^T u(z)$ with $u(z) = u_0 \exp \int_0^z dz' [\Delta(z') - m(z')]$ and u_0 a normalization constant. The associated field operator

$$\hat{\psi}_0 = \int u(z)[f(z) - g(z) + f^\dagger(z) - g^\dagger(z)] dz, \quad (8)$$

has the property $\hat{\psi}_0^\dagger = \hat{\psi}_0$ and represents, therefore, a Majorana fermion.

The above explicit calculation establishes the existence of an unpaired Majorana mode at a SC/magnetic domain wall in a TI nanowire under very special conditions. We now argue that the effect is in fact generic. First, we reason that the magnetic order, although convenient in the derivation, is in fact irrelevant. Consider a nanowire of length $L \gg \xi$, the lengthscale of the zero mode, with the domain wall located near its center. In a physical system Majoranas always come in pairs. Since the second Majorana fermion evidently cannot live in the gapped bulk (or at the magnetic end) we conclude that it must be localized at the SC end, irrespective of the exact boundary condition. Second, it is easy to see that the chemical potential can be moved away from zero without perturbing the Majoranas. Indeed, with $m = 0$ the spectrum of Eq. (6) reads $E_k = \pm[(k \pm \mu)^2 + \Delta_0^2]^{1/2}$ indicating that the bulk of the wire shows a SC gap Δ_0 for any value of μ . Therefore, Majorana end-states will persist even as μ is varied away from 0. When the chemical potential intersects additional bands then each band contributes a single Majorana end-state. Any even number of these will pair up to form ordinary fermions (whose energies will generically be non-zero) but for an odd number of occupied bands a single unpaired zero-energy Majorana will remain. This consideration elucidates the physical meaning of Kitaev's Majorana number \mathcal{M} . We note that the topological nature of the zero mode guarantees its stability against smooth deformations of the nanowire shape, as long as its bulk remains gapped and the total magnetic flux seen by the surface state is unchanged.

To explicitly address the existence and robustness of Majorana end-states we now study the nanowire using

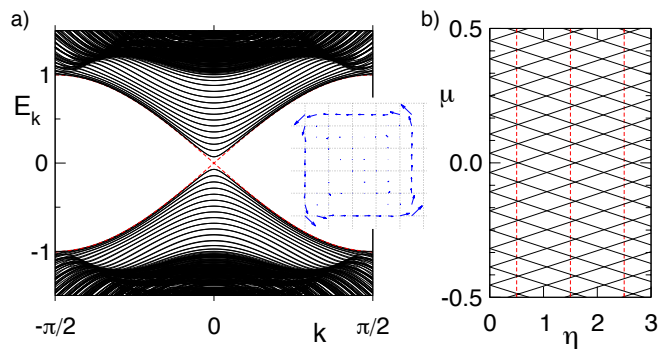


FIG. 3: a) Energy dispersion for an infinitely long TI wire with 20×20 base described by lattice Hamiltonian (9) in the normal state with $\eta = 0.52$. For clarity only the low-energy portion of the spectrum is displayed in a part of the Brillouin zone. Inset shows the spin expectation values for the gapless state at small positive k . The length of the arrow is proportional to the wavefunction amplitude. b) Lines separating regions with different Majorana number $\mathcal{M} = -1(+1)$ extracted from the spectrum. All energies are in units of $\lambda = 150\text{meV}$ and we use parameters $\lambda_x = t = 1$, $\epsilon = 4$ and $g = 32$, corresponding to the strong TI phase with Z_2 index (1;000) and bulk bandgap $2\lambda = 300\text{meV}$.

a concrete lattice model of Bi_2Se_3 family of materials¹⁸. Specifically, we use the model given by Fu and Berg²⁵ regularized on a simple cubic lattice, defined by a k -space Hamiltonian

$$h_{\mathbf{k}} = M_{\mathbf{k}} \sigma_1 + \lambda \sigma_3 (s_2 \sin k_x - s_1 \sin k_y) + \lambda_z \sigma_2 \sin k_z, \quad (9)$$

with $M_{\mathbf{k}} = \epsilon - 2t \sum_{\alpha} \cos k_{\alpha}$. Here σ_{α} represent the Pauli matrices acting in the space of two independent orbitals per lattice site. For $\lambda, \lambda_z > 0$ and $2t < \epsilon < 6t$ the system described by Hamiltonian (9) is a TI in Z_2 class (1;000), i.e. a strong topological insulator. The magnetic field enters through the Peierls substitution, replacing all hopping amplitudes as $t_{ij} \rightarrow t_{ij} \exp[-(2\pi i/\Phi_0) \int_i^j \mathbf{A} \cdot d\mathbf{l}]$ and the Zeemann term $-g\mu_B \mathbf{B} \cdot \mathbf{s}/2$ where $\mu_B = e\hbar/2m_e c$ is the Bohr magneton. In the SC state the BdG Hamiltonian takes the form of Eq. (5) with $\Delta_{\mathbf{k}} = \Delta_0 i s_2$ describing on-site spin singlet pairing.

We have solved the problem posed by Hamiltonian (9) in various wire geometries by exact numerical diagonalization and by sparse matrix techniques. Fig. 3a shows a typical example of the excitation spectrum in an infinitely long wire with $W \times W$ cross-section in the normal state. We observe that for η close to $1/2$ the surface state is indeed gapless and the low-energy modes exhibit the expected pattern of degeneracy. Because of the surface state penetration into the TI bulk the surface electrons see a slightly smaller magnetic flux than the nominal flux $\Phi = BW^2$ given by the wire geometry and the gapless state is shifted to a slightly higher value of η . This is also seen in Fig. 3b which displays the Majorana number for the same system. This figure indicates that for $\eta = 0.52(2n + 1)$ the system will be a 1D topological SC

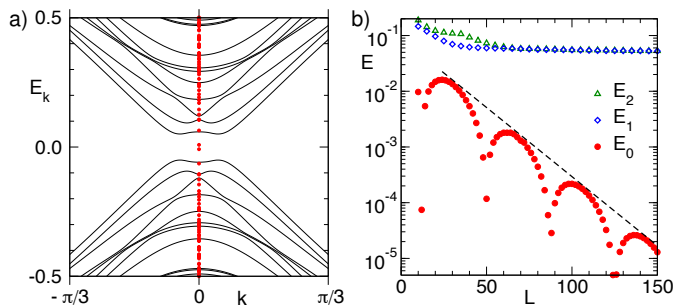


FIG. 4: a) Energy bands for an infinitely long TI wire with 6×6 base in the SC state with $\eta = 0.49$, $\mu = 0.09$, $\Delta_0 = 0.08$ and $g = 0$ (solid lines), and the energy levels for $L = 36$ finite-length wire with open boundary conditions (red circles) obtained by exact numerical diagonalization. b) Three lowest positive energy eigenvalues obtained by the Lanczos method as a function of L . Dashed line represents the envelope function $0.089e^{-L/\xi}$ with $\xi = 17.5$.

for any value of μ inside the bulk gap.

Superconducting order opens a gap in the electron excitation spectrum as illustrated in Fig. 4a. For an open-ended wire, crucially, our calculations reveal a pair of non-degenerate states at $\pm E_0$ inside the SC gap whose energies approach zero for large L as $E_0 \propto e^{-L/\xi}$. Fig. 4b illustrates this exponential decay (which is in addition modulated by oscillations at $2k_F$). Higher energy eigenstates approach non-zero values close to Δ_0 for large L . We have verified that the appropriate linear superpositions of the wavefunctions associated with the $\pm E_0$ eigenvalues are exponentially localized near the ends of the wire. The corresponding field operators then satisfy the Majorana condition $\hat{\psi}^\dagger = \hat{\psi}$, and represent, up to exponentially small corrections in their separation, the Majorana zero modes.

We conclude with comments on the experimental realization. For the existing Bi_2Se_3 nanowires^{13,14} with cross-sectional area $S \approx 6 \times 10^{-15} \text{m}^2$ the surface level spacing is $\delta E_S \simeq v\hbar\sqrt{\pi/S} \simeq 7 \text{meV}$. At half flux quan-

tum, which corresponds to the magnetic field strength $B = \Phi_0/2S \simeq 0.34 \text{T}$, the Zeemann energy scale $\delta E_Z = g\pi\hbar^2/2m_eS \simeq 0.6 \text{meV}$ (taking $v = 5 \times 10^5 \text{m/s}$ and $g = 32$) and thus probably negligible. Experiments on planar Sn- Bi_2Se_3 interfaces¹⁵ show induced SC gap $\sim 0.2 \text{meV}$, a significant fraction of the native Sn bulk gap ($\sim 0.6 \text{meV}$). It thus appears conceivable that a pairing gap of several meV could be induced in Bi_2Se_3 nanowires by using in place of Sn a superconductor with larger bulk gap, such as NbTiN or MgB_2 . A gap of this size should permit detection of the Majorana fermion by scanning tunnelling techniques. The latter will show up as a zero-bias peak exponentially localized near the end of the wire in the topological phase, but will disappear as the phase boundary into non-topological phase is traversed by tuning either chemical potential or magnetic field. Unambiguous detection of Majorana fermions can be achieved by probing 4π -periodic Josephson current through a weak link in the wire as described in Refs.^{10–12}. Another intriguing possibility is to fabricate nanowires from $\text{Cu}_x\text{Bi}_2\text{Se}_3$ which becomes a superconductor below 4K ²⁶ while simultaneously retaining the protected surface states²⁷.

Energy scales order of magnitude higher compared to the ordinary semiconductor wires, significantly reduced requirements for the chemical potential control and the sample purity (afforded by operation in the \mathcal{T} -invariant regime) make TI nanowires promising candidates for the first experimental detection of Majorana fermions. Our numerical simulations of the model Hamiltonian (9) with disorder (to be reported separately) show essential robustness against non-magnetic impurities²⁸ but systematic studies of the effects of disorder and interactions along the lines of recent works^{29,30} constitute an exciting future research direction.

The authors are indebted to J. Alicea, P. Brouwer, S. Frolov, L. Fu, I. Garate, G. Refael, and X.-L. Qi for valuable comments and discussions. The work was supported by NSERC and CIFAR.

¹ E. Majorana, *Nuovo Cimento* **14**, 171 (1937).

² F. Wilczek, *Nature Physics* **5**, 614 (2009).

³ M. Franz, *Physics* **3**, 24 (2010).

⁴ A. Stern, *Nature (London)* **464**, 187 (2010).

⁵ A. Kitaev, *Ann. Phys.* **303**, 2 (2003).

⁶ C. Nayak *et al.*, *Rev. Mod. Phys.* **80**, 1083 (2008).

⁷ L. Fu and C.L. Kane, *Phys. Rev. Lett.* **100**, 096407 (2008).

⁸ J.D. Sau, R.M. Lutchyn, S. Tewari and S. Das Sarma, *Phys. Rev. Lett.* **104**, 040502 (2010).

⁹ J. Alicea, *Phys. Rev. B* **81**, 125318 (2010).

¹⁰ R.M. Lutchyn, J.D. Sau and S. Das Sarma, *Phys. Rev. Lett.* **105**, 077001 (2010).

¹¹ Y. Oreg, G. Refael and F. von Oppen, *Phys. Rev. Lett.* **105**, 177002 (2010).

¹² A.Y. Kitaev, *Phys. Usp.* **44**, 131 (2001).

¹³ H. Peng *et al.*, *Nature Mat.*, **9**, 225 (2010).

¹⁴ H. Tang *et al.*, *ACS Nano* **5**, 7510 (2011).

¹⁵ F. Yang *et al.*, arXiv:1105.0229

¹⁶ J. E. Moore, *Nature* **464**, 194 (2010).

¹⁷ M.Z. Hasan, C.L. Kane, *Rev. Mod. Phys.* **82**, 3045 (2010).

¹⁸ X.-L. Qi, S.-C. Zhang, *Rev. Mod. Phys.* **83**, 1057 (2011).

¹⁹ P. M. Ostrovsky, I. V. Gornyi, A. D. Mirlin, *Phys. Rev. Lett.* **105**, 036803 (2010).

²⁰ G. Rosenberg, H.-M. Guo, and M. Franz, *Phys. Rev. B* **82**, 041104 (2010).

²¹ J.H. Bardarson, P.W. Brouwer, and J.E. Moore, *Phys. Rev. Lett.* **105**, 156803 (2010).

²² Y. Zhang and A. Vishwanath, *Phys. Rev. Lett.* **105**, 206601 (2010).

²³ A.C. Potter and P.A. Lee, *Phys. Rev. B* **83**, 184520 (2011).

- ²⁴ R. Jackiw and P. Rossi, Nucl. Phys B **190**, 681 (1981).
- ²⁵ L. Fu and E. Berg, Phys. Rev. Lett. **105** 097001, (2010).
- ²⁶ Y.S. Hor *et al.*, Phys. Rev. Lett. **104**, 057001 (2010).
- ²⁷ L.A. Wray *et al.*, Nature Phys. **6**, 855 (2010).
- ²⁸ A. Cook and M. Franz, (unpublished).
- ²⁹ See e.g. P.W. Brouwer *et al.*, arXiv:1103.2746
- ³⁰ See e.g. E.M. Stoudenmire *et al.*, Phys. Rev. B **84**, 014503 (2011).